Cryptic speciation of benthic *Prorocentrum* (Dinophyceae) species and their potential as ecological indicators

Yixuan Wu [a,b], Shuning Huang [b], Bernd Krock [c], Chui Pin Leaw [d], Sing Tung Teng [e], Ajcharaporn Piumsomboon [f], Porntep Punnarak [g], Kakaskasen Andreas Roeroe [h], Na Wang [b], Haifeng Gu [b,i,*]

[a] *Fisheries College, Jimei University, Xiamen 361021, China*
[b] *Third Institute of Oceanography, Ministry of Natural Resources, Xiamen 361005, China*
[c] *Alfred Wegener Institut–Helmholtz Zentrum für Polar– und Meeresforschung, Am Handelshafen 12, D–27570 Bremerhaven, Germany*
[d] *Bachok Marine Research Station, Institute of Ocean and Earth Sciences, University of Malaya, 16310 Bachok, Kelantan, Malaysia*
[e] *Faculty of Resource Science and Technology, Universiti Malaysia Sarawak, 94300 Kota Samarahan, Sarawak, Malaysia*
[f] *Maritime Administration Program, Graduate School, Chulalongkorn University, Bangkok 10330, Thailand*
[g] *Aquatic Resources Research Institute, Chulalongkorn University, Bangkok 10330, Thailand*
[h] *Sam Ratulangi University, Sulawesi Utara, Manado 95115, Indonesia*
[i] *Key Laboratory of Marine Ecological Conservation and Restoration, Ministry of Natural Resources, Xiamen 361005, China*

ARTICLE INFO

ABSTRACT

The response of marine ecosystems to rapid climate changes has been well recognized but not studied extensively. Benthic microalgae, in contrast to the phytoplankton that is able to be transported by currents, have limited dispersal ability and thus are a better ecological indicator to climate changes. Here we performed sampling in the Yellow Sea, the East China Sea and South China Sea and established twenty-six strains of benthic *Prorocentrum* for detailed morphological and molecular examinations. Five *Prorocentrum* species, including *P. concavum*, *P. fukuyoi*, *P. mexicanum*, *P. tsawwassenense*, and *P.* cf. *sculptile*, were identified. Both *P. concavum* and *P. fukuyoi* displayed marked intraspecific divergences in large subunit (LSU) ribosomal RNA gene sequences, corresponding to their geographical origins. In contrast, *P. mexicanum* strains shared identical LSU sequence. *Prorocentrum tsawwassenense* and *P.* cf. *sculptile* are not suitable ecological indicators as they were rarely observed. *Prorocentrum mexicanum* is not recommended either as it is present across the region. In contrast, *P. concavum* and *P. fukuyoi* have advantages as ecological indicators for climate changes in the Western Pacific as they comprise several ribotypes with differentiated biogeography. Toxin analysis was also performed on all five species except *P. fukuyoi* by liquid chromatography coupled to tandem mass spectrometry, but okadaic acid was not detectable.

1. Introduction

Global surface temperature has been increasing with a record of 1 °C higher in the last decades compared to the beginning of the industrial revolution, and an intermediate scenario projects an increase of 2 °C by 2300 (Masson-Delmotte et al., 2021). As a response to global warming, marine taxa moved poleward with an average rate of 70 km each decade (Poloczanska et al., 2013). Climate-driven species redistribution at both regional and global scales is expected to have profound consequences for ecosystem structure and function (Pecl et al., 2017). The geographic range of species is regarded as the basic unit of biogeography and refers to the area where the species is present (Brown et al., 1996). The diversity, abundance, growth rate of one or more species in a specific site reflect the effects of current and past environmental changes, and thus identification of easily monitored ecological indicators helps to track or predict the environmental conditions where they are found (Burger, 2006).

Phytoplankton has high biomass and dispersal potential, and poleward dispersal has been predicted using mechanistic species distribution models (Thomas et al., 2012), and observed during long-term

---

monitoring. For example, the toxic dinophyte *Alexandrium minutum* was considered to colonize the North Sea in the 1980ies, which was originally present in the Mediterranean Sea only (Nehring, 1998). *Alexandrium pseudogonyaulax* and *Alexandrium catenella* were not dominant in the North Sea (Kremp et al., 2019), and in the Arctic (Anderson et al., 2021) until recently. In contrast to these planktonic dinophyte species, benthic dinophytes have low dispersal potential, thus may offer better chances for an ecological indicator of climate change (Tester et al., 2020; Drouet et al., 2021). However, detailed investigations on the diversity and distribution of benthic dinophytes are still limited, especially in subtropical and temperate areas.

The dinophyte genus *Prorocentrum* includes 84 formally accepted species (Guiry and Guiry, 2022). The majority of *Prorocentrum* are planktonic but approximately 30 of them are benthic or epibenthic (Hoppenrath et al., 2013; Nascimento et al., 2017). These *Prorocentrum* species often inhabit intertidal marine sediments (Faust, 1994; Hoppenrath, 2000), but they can inhabit seagrass, macroalgae, floating detritus or corals as well (Fukuyo, 1981; Faust, 1990; Faust, 1993; Grzebyk et al., 1998). The main features to classify *Prorocentrum* species include the shape and size of cells, surface morphology of thecal plates (e.g., pore sizes and patterns), morphology of intercalary band and the periflagellar area (Hoppenrath et al., 2013).

The precise identity of certain benthic *Prorocentrum* species remains elusive. *Prorocentrum maculosum* is not considered a synonym of *P. hoffmannianum* until recently (Rodríguez et al., 2018). Moreover, molecular sequences of several *Prorocentrum* species from the type locality are still missing, such as *P. emarginatum* and *P. sculptile*. On the other hand, some *Prorocentrum* species are rarely reported since the original description (e.g., *P. tsawwassenense*, Hoppenrath and Leander, 2008; Kim et al., 2015).

Investigation of benthic *Prorocentrum* species in the Western Pacific dated back to the pioneering work using light microscopy on specimens from Ryukyu Islands, Japan (Fukuyo, 1981), and later using scanning electron microscopy on samples collected from Vietnam (Larsen and Nguyen, 2004), East Malaysia and Peninsula Malaysia (Mohammad-Noor et al., 2007a), and from the Gulf of Thailand (Piumsomboon et al., 2001). However, molecular sequences were not provided in these studies. Subsequent surveys were performed combining morphology and molecular characterization of samples collected from Dongho, Korea (Kim et al., 2015), Hainan, China (Luo et al., 2017; Zou et al., 2021), Perhentian Island, Malaysia (Lim et al., 2019), and Japan (Nishimura et al., 2020a; Nishimura et al., 2020b). Detailed examinations on benthic *Prorocentrum* species in many parts of the Western Pacific, such as northern China and Indonesia, are still missing.

Some *Prorocentrum* species have been reported to generate okadaic acid (OA) and related derivatives (dinophysistoxins, DTXs); these toxins were believed to cause diarrheic shellfish poisoning (DSP). OA production is known in *P. caipirignum* (Nascimento et al., 2017; Lim et al., 2019), *P. lima* (Murakami et al., 1982; Lim et al., 2019), *P. concavum* (Dickey et al., 1990), *P. steidingerae* (as *P. rhathymum*) (An et al., 2010), *P.* cf. *fukuyoi* (Nishimura et al., 2020b), *P. hoffmannianum* (Morton and Bomber, 1994), *P. leve* (Faust et al., 2008), and *P. belizeanum* (Morton et al., 1998). OA production in many epibenthic *Prorocentrum* species has not yet been examined and may help to differentiate closely related species or cryptic species.

Cryptic diversity has been reported in the benthic *Prorocentrum lima* and *P. fukuyoi* (Zhang et al., 2015; Chomérat et al., 2018). Whether this cryptic diversity are related to geographic origins is not clear, and cryptic speciation in other benthic *Prorocentrum* species has not been fully investigated. In addition, the previous ecological indicator for climate change is based on species only but a high-resolution indicator at the molecular level will be more powerful. Therefore, the present study aims to: (1) understand the biogeography and potential genetic differentiation of benthic *Prorocentrum* in the Western Pacific; and (2) identify potential coastal ecological indicators for climate change in this region. We performed sampling across the East and South China Sea, the

Yellow Sea, and established 26 strains of *Prorocentrum* species. All of them were subjected to morphological and molecular analysis and five species were identified. DSP toxin analysis was also performed on five strains of four species by liquid chromatography with tandem mass spectrometry (LC–MS/MS).

2. Materials and methods

2.1. Sample collection and treatment

Sand samples were collected by a polycarbonate bottle together with seawater during low tide or by SCUBA divers in the Yellow Sea, the East China Sea and South China Sea between 2015 and 2020 (Table 1, Fig. 1). The samples were stirred vigorously and the detached cells were transferred into a Petri dish. In addition, a water sample was collected during an *Akashiwo sanguinea* bloom in Kelantan, Malaysia in 2017. Single *Prorocentrum* like cells were isolated with a micropipette using a Motic AE31 inverted microscope (Motic, Xiamen, China), and transferred into 96 well plates full of f/2–Si medium (Guillard and Ryther, 1962). Twenty-six strains were able to grow at 20 or 25 °C (depending on the origins), 90 $\mu E \cdot m^{-2} \cdot s^{-1}$ with a 12:12 h light: dark cycle.

2.2. Morphological examination with LM and SEM

Living cells including chloroplast were photographed with a Zeiss Axio Imager light microscope (Carl Zeiss, Göttingen, Germany), equipped with a Zeiss Axiocam HRc digital camera at 400× magnification. Measurement of cell size was performed with Axiovision v.4.8.2 software. The nucleus were stained using Sybr Green (Sigma Aldrich, St. Louis, USA) and photographed with the above microscope.

Cells were concentrated by centrifugation by a Universal 320 R centrifuge (Hettich–Zentrifugen, Tuttlingen, Germany) at 2701*g* for 10 min. Cells were fixed with 2.5% glutaraldehyde for 60 min and then moved to a coverslip coated with poly-L-lysine. The samples were washed with deionized water (Milli-Q, Sartorius, Göttingen, Germany) twice and dehydrated, critical point dried and sputter–coated with gold as described previously (Luo et al., 2017). Cells were photographed using a Zeiss Sigma FE scanning electron microscope (Carl Zeiss, Oberkochen, Germany). Terminology for morphological description follows Hoppenrath et al. (2013).

2.3. Gene amplification and sequencing

Single cells were cleaned with deionized water repeatedly. The cells were crushed with a coverslip and directly used as a template. Gene amplifications were performed in a 50 μL reaction system, which contains 1 × PCR buffer, 0.2 μM of each primer, 50 μM dNTP mixture, and 1 U of ExTaq DNA Polymerase (Takara, Tokyo, Japan). The partial LSU ribosoma RNA (D1–D6) gene and/or internal transcribed spacer (ITS) region were amplified using a Mastercycler (Eppendorf, Hamburg, Germany) as described in Luo et al. (2017). The amplicons were purified with a DNA Gel Extraction Kit (Sangon Biotech, Shanghai, China) and sequenced on an ABI PRISM 3730XL (Applied Biosystems, Foster City, CA, USA) in each direction. Sequences obtained in this study were deposited in GenBank (accession numbers: OP764407 to OP764433).

2.4. Sequence alignment and phylogenetic analysis

New sequences were incorporated into downloaded LSU rRNA gene sequences of *Prorocentrum* from the GenBank. The sequences were aligned by MAFFT v7.110 (Katoh and Standley, 2013) with the default settings. Sequence similarity was obtained by BioEdit v. 7.0.5 (Hall, 1999).

The best model chosen by jModelTest (Posada, 2008) with Akaike Information Criterion was used in Bayesian inference (BI) and maximum likelihood (ML). BI was carried out with MrBayes 3.2 (Ronquist and

Table 1

Information on *Prorocentrum* strains examined in this study, including species, strains, the collection date, latitude, longitude and origins.

| Species	Strains	Collection date	Latitude	Longitude	Origins
P. tsawwassenense	TIO304	Oct. 14, 2015	36°3′6.9″N	120°21′49.62″E	Qingdao, Shangdong, China
P. fukuyoi	TIO305	Sep. 14, 2015	36°3′6.9″N	120°21′49.62″E	Qingdao, Shangdong, China
P. fukuyoi	TIO915	April 13, 2018	24°53′1.78″N	118°54′56.85″E	Quanzhou, Fujian, China
P. fukuyoi	TIO942	Dec. 25, 2018	11°49′46.82″N	102°28′57.54″E	Trat, Thailand
P. fukuyoi	TIO952	June 2, 2019	26°42′1.87″N	120°6′23.11″E	Ningde, Fujian, Chinaa
P. fukuyoi	TIO970	June 2, 2019	26°42′1.87″N	120°6′23.11″E	Ningde, Fujian, China
P. cf. *sculptile*	TIO968	May 27, 2019	1°46′1.7″N	125°2′22.2″E	Manado, Indonesia
P. concavum	TIO892	Nov. 9, 2017	19°29′40.71″N	110°48′32.72″E	Wenchang, Hainan,China
P. concavum	TIO917	Nov. 21, 2017	13°7′27.89″N	100°48′33.42″E	Sichang, Thailand
P. concavum	TIO925	Aug. 22, 2018	10°33′20.47″N	99°22′34.06″E	Chumphon, Thailand
P. concavum	TIO933	Aug. 17, 2018	10°41′55.75″N	99°24′29.18″E	Chumphon, Thailand
P. concavum	TIO941	May 27, 2019	1°46′1.7″N	125°2′22.2″E	Manado, Indonesia
P. mexicanum	TIO241	Mar. 4, 2015	24°26′55.55″N	118°9′50.61″E	Xiamen, Fujian, China
P. mexicanum	TIO458	May 26, 2017	6°1′17.41″N	102°25′18.32″E	Kelantan, Malaysia
P. mexicanum	TIO497	July 10, 2017	10°41′55.75″N	99°24′29.18″E	Chumphon, Thailand
P. mexicanum	TIO602	Aug. 22, 2018	10°33′20.47″N	99°22′34.06″E	Chumphon, Thailand
P. mexicanum	TIO603	Aug.t 22, 2018	10°33′20.47″N	99°22′34.06″E	Chumphon, Thailand
P. mexicanum	TIO604	Aug. 22, 2018	10°33′20.47″N	99°22′34.06″E	Chumphon, Thailand
P. mexicanum	TIO898	Dec. 25, 2018	11°49′46.82″N	102°28′57.54″E	Trat, Thailand
P. mexicanum	TIO932	Aug. 17, 2018	10°41′55.75″N	99°24′29.18″E	Chumphon, Thailand
P. mexicanum	TIO947	Dec. 25, 2018	11°49′46.82″N	102°28′57.54″E	Trat, Thailand
P. mexicanum	TIO953	June 2, 2019	25°7′39.79″N	118°56′46.87″E	Putian, Fujian, China
P. mexicanum	Asm1610 PrB10	Oct. 16, 2017	1° 40′ 42.28″N	110°20′15.23″E	Kuching, Sarawak, Malaysia
P. mexicanum	LBsPr2210C4	Oct. 22, 2017	1° 36′ 31.65″N	110°19′ 6.53″E	Kuching, Sarawak, Malaysia
P. mexicanum	JSbPr1310G5	Oct. 13, 2017	1° 42′ 59.85″N	110°19′ 1.68″E	Kuching, Sarawak, Malaysia
P. mexicanum	SBSC10	Oct. 22, 2020	1° 36′ 31.65″N	110°19′ 6.53″E	Kuching, Sarawak, Malaysia
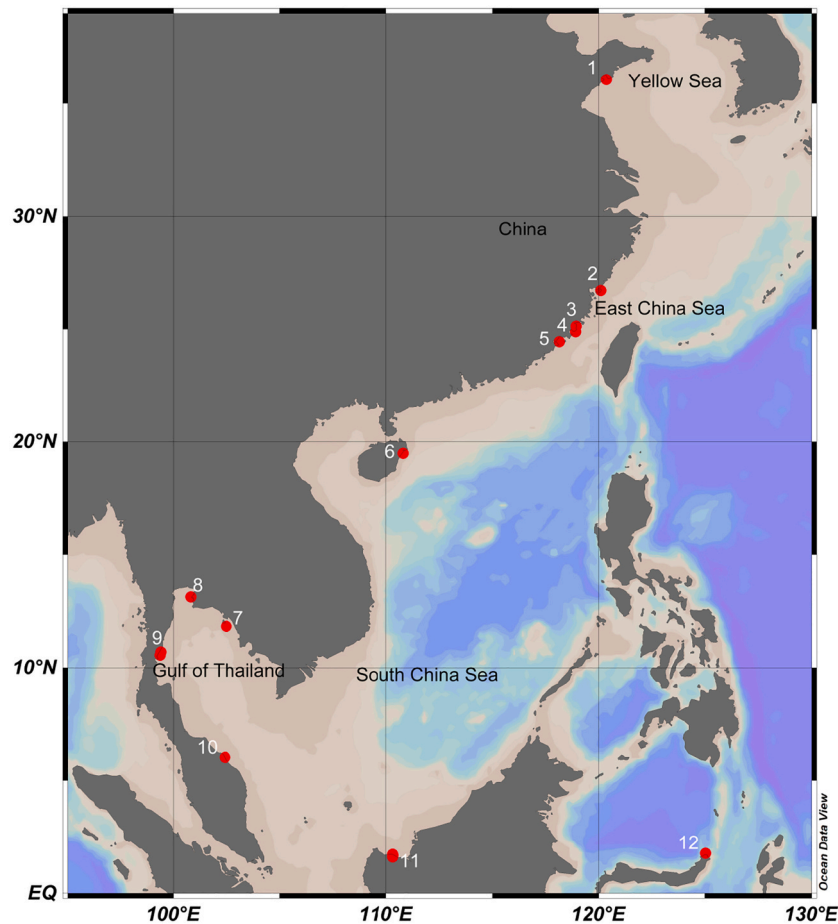
Fig. 1. Map of sampling stations in the Western Pacific. 1: Qingdao, Shandong, China; 2: Ninde, Fujian, China; 3: Putian, Fujian, China; 4: Quanzhou, Fujian, China; 5: Xiamen, Fujian, China; 6: Wenchang, Hainan, China; 7: Trat, Thailand; 8: Sichang, Thailand; 9: Chumphon, Thailand; 10: Kelantan, Malaysia; 11: Kuching, Sarawak, Malaysia; 12: Manado, Indonesia.

Huelsenbeck, 2003). Four Markov chain Monte Carlo (MCMC) chains were carried out for 2,000,000 generations, with a sampling every 1000 generations. The first 200,000 generations were discarded as the burn-in. The posterior probabilities of each clade was assessed by reconstructing a majority-rule consensus tree. ML was carried out with RaxML v.7.2.6 (Stamatakis, 2006) using the T–REX web server (Boc et al., 2012). 1000 bootstrap replications were preformed to assess the clade support.

2.5. Toxin analysis

Approximately 10^4–10^6 cells of *Prorocentrum* strains TIO214, TIO304, TIO497, TIO941, and TIO968 were harvested using the the above centrifuge at 2701 *g* for 10 min at 4 °C. Toxin extraction followed the procedures detailed in Luo et al. (2017). Toxin analysis was performed by LC-MS/MS, as described in detail previously (Krock et al., 2008). The quantity of okadaic acid was calibrated with a standard solution purchased from the National Research Council, Halifax, NB, Canada. The detection limit was determined as 24 pg per sample based on a signal-to-noise ration of 3.

3. Results

3.1. Morphological characterization

Twenty-six strains of *Prorocentrum* were established in present study, fourteen were identified as *P. mexicanum,* five strains each were identified as *P. fukuyoi* and *P. concavum*, and one strain each was identified as *P. tsawwassenense* and *P.* cf. *sculptile*, respectively (Table 1). Cell of all *Prorocentrum* strains were dorsoventrally flattened and described below.

3.1.1. Prorocentrum concavum

Cells of strain TIO941 from Indonesia were symmetric and broad ovoid. They were 43.6–48.9 μm long (45.9 ± 1.6 μm, *n* = 30) and 36.6–43.5 μm wide (39.8 ± 1.6 μm, n = 30). The ratio of length and width varied from 1.10 to 1.20 (1.16 ± 0.03, n = 30). The nucleus was slightly elongated and positioned posteriorly (Fig. 2A). Two cup-shaped pusules were present in the anterior. A central pyrenoid with a starch ring was observed with many radiating chloroplasts (Fig. 2A, B, C). The thecal surface was full of oval to round depressions (0.56–0.87 μm in diameter) and ornamented with pores inside, which was absent in the center (Fig. 2B, D, E).The periflagellar area was wide V-shaped with nine platelets (Fig. 2F). The flagella pore (fp) was large but the accessory pore (ap) was small (Fig. 2F). Cells of strain TIO933 from Thailand were morphologically identical to strain TIO941.

3.1.2. Prorocentrum fukuyoi

Cells of strain TIO305 from the Yellow Sea were slightly asymmetric, oval to oblong (Fig. 3A, E). They were 26.2–37.9 μm long (29.3 ± 3.2 μm, *n* = 50) and 17.0–25.0 μm wide (21.9 ± 2.2 μm, n = 50). The ratio of length and width varied from 1.2 to 1.6 (1.40 ± 0.10, n = 50). The nucleus was round and situated posteriorly. A central pyrenoid with a starch ring was observed with many radiating chloroplasts (Fig. 3B). The thecal plate was smooth and had pores of two sizes. Large pores (0.20–0.27 μm in diameter) formed short radial rows toward the center at times (Fig. 3C, D). Small pores (0.07–0.10 μm in diameter) were scattering and much denser in the periphery. The central part was devoid of pores. The periflagellar area was V-shaped, deep and narrow with nine platelets (Fig. 3F). The fp was large but the ap was small, and separated by a short list (Fig. 3F).

3.1.3. Prorocentrum mexicanum

Cells of *P. mexicanum* strain TIO604 from Thailand were asymmetric and oblong (Fig. 4A). They were 26.7–36.4 μm long (30.4 ± 1.9 μm, *n* = 41) and 17.5–23.3 μm wide (20.4 ± 1.7 μm, n = 41). The ratio of length and width varied from 1.31 to 1.83. The nucleus was elongated and situated posteriorly (Fig. 4B). Chloroplasts were observed in the periphery (Fig. 4A). The thecal plates were smooth and had pores of two sizes. The large pores (0.5–0.6 μm in diameter) formed radial rows (Fig. 4C and D). The periflagellar area was shallow and wide V-shaped with nine platelets (Fig. 4E). There was a marked wing in platelet 1 (Fig. 4D).

3.1.4. Prorocentrum cf. sculptile

Cells of strain TIO968 from Indonesia were symmetric and broad oval to ovoid (Fig. 5A). They were 36.4–47.5 μm long (42.4 ± 2.9 μm, *n*
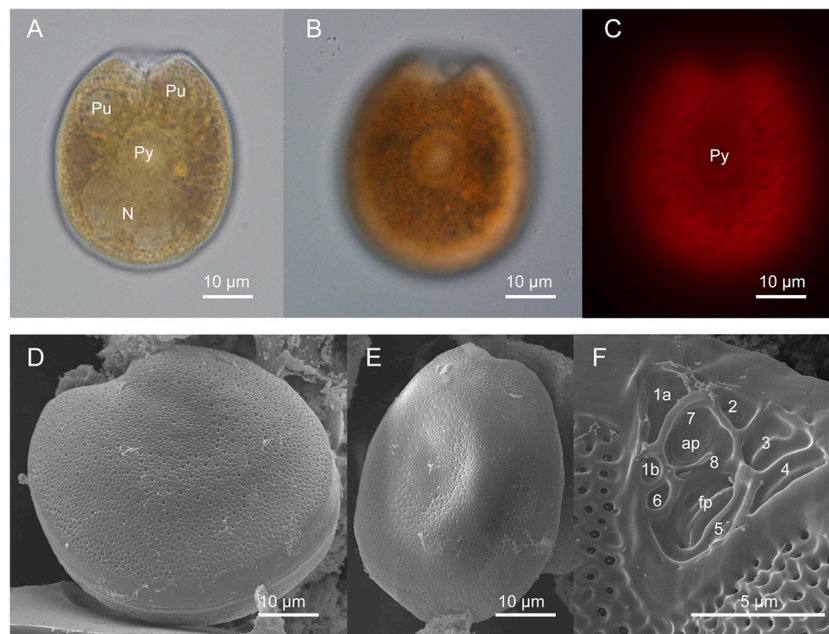

Fig. 2. LM and SEM of *Prorocentrum concavum* cells. (A) A living cell showing the nucleus (N), pyrenoid (Py), two pusules (Pu), and the V-shaped periflagellar area; (B) A living cell, showing the depressions on the thecal surface; (C) Autofluorescence of a living cell showing a pyrenoid (Py) and network of chloroplasts. (D, E) Right and left thecal view, showing numerous depressions. (F) The detail of periflagellar area, showing nine platelets, the flagella pore (fp) and accessory pore (ap).
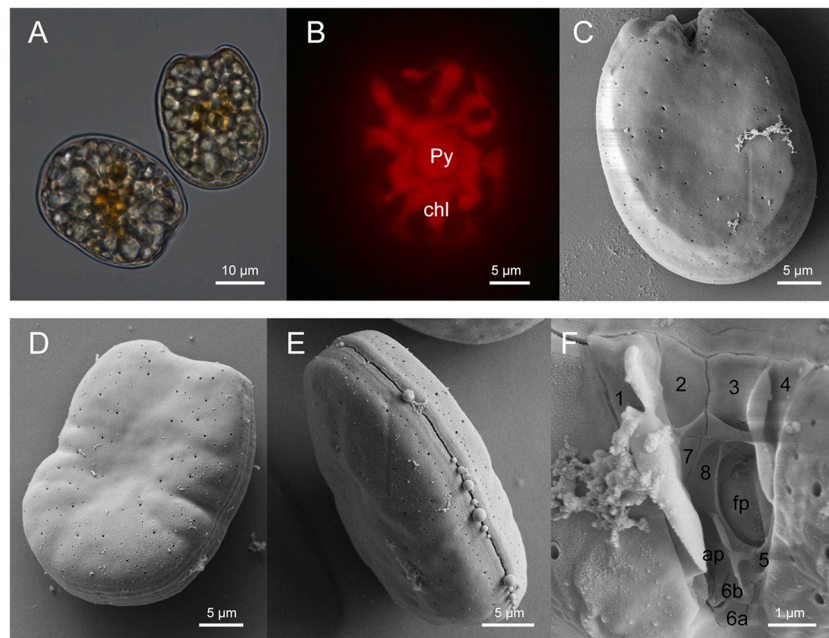
Fig. 3. LM and SEM of *Prorocentrum fukuyoi* cells. (A) Two cells of variable shape. (B) Autofluorescence of a living cell, showing a pyrenoid (Py) and radiating chloroplasts (chl). (C) A living cell, showing the V-shaped periflagellar area; (D) Left thecal view showing pores of two sizes. (E) Lateral view showing intercalary band. (F) The detail of periflagellar area.
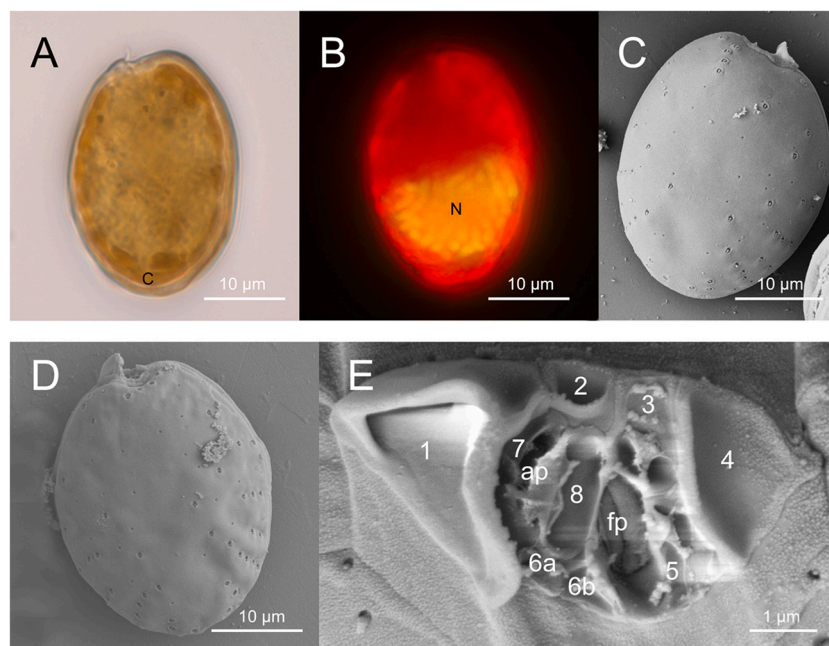

Fig. 4. LM and SEM of *Prorocentrum mexicanum* cells. (A) A living cell in right thecal view, showing the chloroplasts (C). (B) Autofluorescence of a living cell, showing the nucleus (N). (C) View of left theca, showing pores of two sizes. (D) View of right theca, showing the wide V-shaped periflagellar area and a pronounced wing. (E) The detail of periflagellar area.

= 38) and 33.9–43.6 μm wide (36.9 ± 1.0 μm, n = 38). The ratio of length and width varied from 1.15 to 1.30 (1.13 ± 0.03, n = 38). The nucleus was elongated and curved, situated posteriorly (Fig. 5A). A central pyrenoid with a starch ring was observed with many radiating chloroplasts (Fig. 5B). The thecal plate was smooth and had large depressions (0.52–0.83 μm in diameter). Thecal pores were arranged radially (Fig. 5C, D). The periflagellar area was V-shaped, deep and narrow with nine platelets (Fig. 5E, F). The fp was large whereas the ap was not observed (Fig. 5E, F).

3.1.5. Prorocentrum tsawwassenense

Cells of strain TIO304 from the Yellow Sea were symmetric and broad ovoid (Fig. 6A). The cells were 42.3–47.4 μm long (44.8 ± 1.2 μm, n = 50) and 35.0–39.0 μm wide (36.9 ± 1.0 μm, n = 50). The ratio of length and width varied from 1.15 to 1.30 (1.21 ± 0.03, n = 50). The nucleus was elongated and curved and situated posteriorly (Fig. 6B). The thecal surface showed radial arranged large pores (0.25–0.31 μm in diameter) but not in the central part (Fig. 6C, D). Smaller pores (0.06–0.18 μm in diameter) were randomly scattering on the surface.
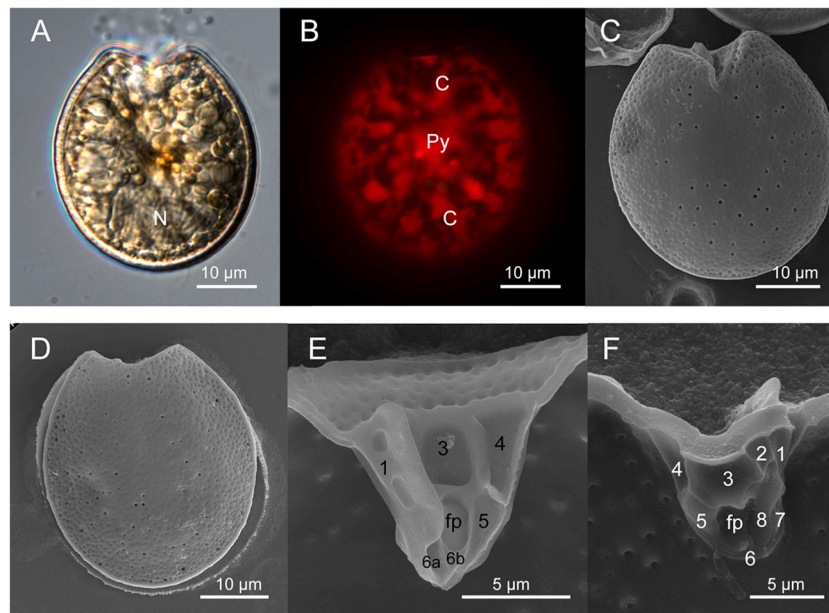
Fig. 5. LM and SEM of *Prorocentrum* cf. *sculptile* cells. (A) A living cell in right thecal view, showing the nucleus (N). (B) Autofluorescence of a living cell, showing the pyrenoid (Py) and chloroplasts (C). (C) View of right theca, showing the deep V-shaped periflagellar area. (D) View of left theca, showing the numerous depressions and large pores. (E, F) The detail of periflagellar area.
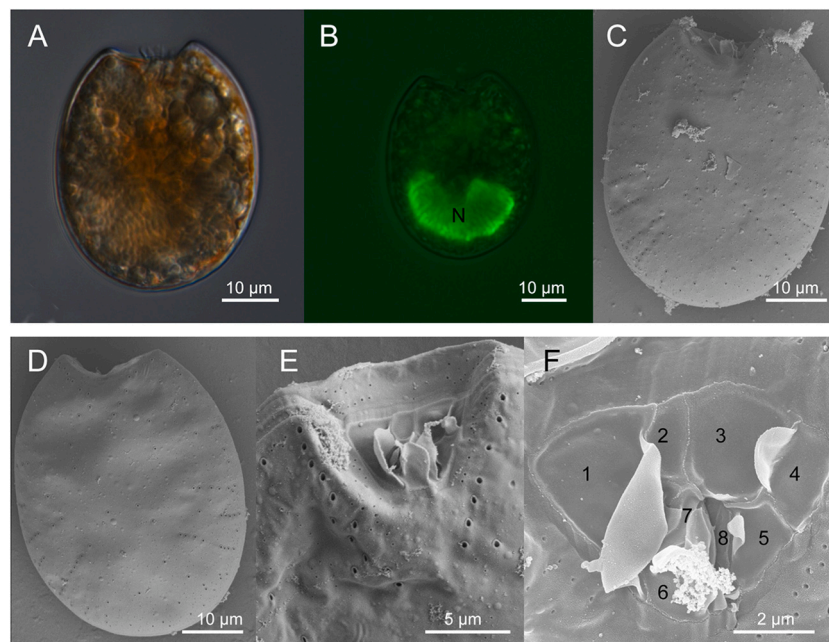

Fig. 6. LM and SEM of *Prorocentrum tsawwassenense* cells. (A) A living cell in right thecal view showing the U-shaped periflagellar area. (B) A cell stained by SYBR Green, showing the nucleus (N). (C, D) Right and left thecal view, showing the radially arranged pores. (E) The periflagellar area, showing the incomplete V-shaped pores. (F) The detail of periflagellar area. (For interpretation of the references to colour in this figure legend, the reader is referred to the web version of this article.)

Either irregular or double rows of large pores formed an incomplete "V" at the apical end (Fig. 6E). The periflagellar area was wide U-shaped with eight platelets and several prominent wings (Fig. 6E, F).

3.2. Molecular characterization and phylogeny

3.2.1. Prorocentrum concavum

Three strains from the Gulf of Thailand (TIO917, TIO925, and TIO933) shared identical LSU rRNA gene sequences. However, they differed from strain TIO892 of Hainan in three positions and from strain TIO941 (Indonesia) and an Australian strain (GenBank no: MH567255) in seven and 14 positions (Table 2). Strain TIO941 shared an identical LSU sequence with strain SP001 (Perhentian Island of Malaysia, GenBank no: ON229478) and differed from strain NMN013 (Sabah, Malaysia, GenBank no: EF566744) in only one position. Strains TIO941 and SP001 shared identical ITS sequence too.

The phylogenetic analyses generated trees with similar topologies using ML and BI. The best ML tree showed that *P. concavum* comprised three clades. Clade B included strains from Gulf of Thailand, Malaysia, Arabian Sea, Caribbean Sea, and Reunion Island with maximal support

Table 2
LSU rDNA (D1–D3) sequence differences (above the diagonal line) and similarity (below the diagonal line) of *Prorocentrum concavum*.

	GenBank no/Strains, origin	1	2	3	4	5	6	7
1	OP764406/TIO892, Hainan, China	–	3	8	4	5	6	11
2	OP764408/TIO925, Thailand	99.6%	–	5	7	8	5	14
3	AJ567464/Reunion Island	99.0%	99.4%	–	12	13	10	17
4	OP764410/TIO941, Indonesia	99.5%	99.1%	98.5%	–	1	8	15
5	MG701855/Caribbean Sea	99.4%	99.0%	98.4%	99.8%	–	9	16
6	MG701854/Caribbean Sea	99.2%	99.4%	98.8%	99.0%	98.9%	–	17
7	MH567255/Australia	98.6%	98.3%	97.9%	98.2%	98.0%	97.9%	–

(ML BS: 100%; BI PP: 1.0). Clade A encompassed strains from Malaysia, Indonesia, and Caribbean Sea with maximal support and Clade C included strains exclusively from Hainan, China with low support. Two strains from Australia and Xisha Island (South China Sea) fell outside these three clades (Fig. 7).

Fig. 7. A maximum likelihood (ML) inferred tree of *Prorocentrum concavum* based on sequences of LSU rRNA gene (D1–D3). Red and bold nodal labels refer to newly obtained sequences. Lengths of branches are painted to scale. The scale bar is equal to the number of nucleotide substitutions per site. Nodal supports are ML bootstrap support (BS) and Bayesian inference posterior probabilities (BI PP). BS <50% and PP <0.9 are not shown. Asterisk refers to maximal support (ML BS: 100; BI PP: 1.0).

3.2.2. Prorocentrum fukuyoi

Strains TIO970 and TIO952 from the same locality (Ningde, East China Sea) shared identical sequences, but the number of sequences dissimilarity ranged from 1 to 194 compared to isolates from elsewhere (Table 3).

The phylogenetic analyses generated trees with similar topologies using ML and BI. The best ML tree demonstrated that *P. fukuyoi* comprised four well-resolved clades. Clade A included the type strain from Australia, a strain from Fiji, and some isolates from Europe with strong support (ML BS: 100%; BI PP: 0.99). Clade B included strains from the Asia Pacific and Arabian Gulf with maximal support. These two clades were a sister of clade C comprising strains from Europe, Kuwait, Hong Kong, Japan, and the Caribbean Sea with low support. They again formed a sister of clade D with strains exclusively from the Caribbean Sea (Fig. 8).

3.2.3. Prorocentrum mexicanum

Prorocentrum mexicanum strains TIO241 and TIO953 from the East China Sea shared identical sequences with those of strains from the Gulf of Thailand (TIO602, TIO603, TIO604, TIO898, TIO932, and TIO947) and strain JSbPr1310G5 from Sarawak. They differed from strains elsewhere from one (99.80%) to seven (99.10%) positions (Table 4).

The phylogenetic analyses generated trees with similar topologies using ML and BI. The best ML tree demonstrated that *P. mexicanum* formed a sister clade of *P. steidingerae* with maximal support. The majority of *P. mexicanum* strains from the Western Pacific and those from Australia, Mexico, Cuba, USA grouped together with strong ML support (63) but low posterior probability. They formed a sister clade to two strains from Kuwait with maximal support (Fig. 9).

3.2.4. Prorocentrum tsawwassenense and Prorocentrum cf. sculptile

Prorocentrum tsawwassenense strain TIO304 differed from a Korean isolate only in one position (99.90% similarity) and differed from those of Kuwait and France in 16, 19 and 114 positions. *Prorocentrum* cf. *sculptile* strain TIO968 differed from those of the Caribbean Sea in 14 positions (98.30% similarity, Table 5). The phylogenetic analyses generated trees with similar topologies using ML and BI. The ML tree demonstrated that *P. tsawwassenense* from the Yellow Sea grouped together with maximal support and was a sister clade of those from Kuwait receiving maximal supports. They again formed a sister clade to French isolates with maximal support. *Prorocentrum* cf. *sculptile* from Indonesia formed a sister clade to those from the Caribbean Sea with maximal support (Fig. 9).

3.3. Toxin production

No OA/DTX were detected in *Prorocentrum concavum* (strain TIO941, <0.0012 pg cell^{-1}), *P. mexicanum* (strains TIO214 and TIO497, <0.0002 pg cell^{-1}), *P. tsawwassenense* (strain TIO304, <0.0076 pg cell^{-1}), and *P.* cf. *sculptile* (strain TIO968, <0.0026 pg cell^{-1}).

3.4. Potential ecological indicator for climate changes

The sampling stations were classified into three climate zones, i.e. temperate, subtropical and tropical zones. Only two species (*P. tsawwassenense* and *P. fukuyoi* ribotype B3) were encountered in temperate zone (station 1). Three species (*P. fukuyoi* ribotype B3, *P. concavum* ribotype C and *P. mexicanum*) were found in subtropical zone (stations 2–6), whereas all species except *P. tsawwassenense* were encountered in tropical zone (stations 7–12, Table 6).

Prorocentrum tsawwassenense and *P.* cf. *sculptile* were rarely found in Western Pacific, thus are not ideal candidates for ecological indicator. *Prorocentrum mexicanum* was only recorded in tropical and subtropical areas (Table 6), thus may serve as the ecological indicator of warm waters. *Prorocentrum fukuyoi* ribotype B3 was recorded in temperate and subtropical areas, but ribotype B4 was only found in tropical areas (Table 6). The latter has the potential as an ecological indicator of warm waters too. *Prorocentrum concavum* ribotypes A and B were recorded in tropical areas, whereas ribotype C was found in subtropical areas (Table 6). All these ribotypes have the potential as ecological indicators of climate change as well.

4. Discussion

4.1. Cryptic speciation of Prorocentrum species

Our limited sampling in the Western Pacific revealed five benthic *Prorocentrum* species, among them *P.* cf. *sculptile* has not been reported in this area before. *P. fukuyoi* and *P. tsawwassenense* are the first records in Thailand and China, respectively. Both *P. concavum* and *P. fukuyoi* show changes in LSU sequences corresponding to geographic origins but *P. mexicanum* does not display any intraspecific sequence divergence.

4.1.1. Prorocentrum concavum

Prorocentrum concavum was firstly described from Ryukyu Island, Okinawa, Japan (Fukuyo, 1981). Our strains from China, Thailand, and Indonesia fit the original descriptions regarding the number and shape of pusules, a wide V-shaped periflagellar area, and patterns of depressions, trichocyst pores, and nine periflagellar platelets.

P. concavum is reported from sand samples (Saburova et al., 2009; present study), as epibenthic on macroalgae, seagrass, or floating detritus (Fukuyo, 1981; Faust, 1990; Grzebyk et al., 1998; Mohammad-Noor et al., 2007b), and even as planktonic (as *P. arabianum*) (Morton et al., 2002; Zou et al., 2020). These behaviors may explain the genetic uniformity among strains in the Gulf of Thailand where relatively short distances (<350 km) were observed. In addition, counterclockwise and clockwise circulation during the southwest and northeast monsoon season in the Gulf of Thailand (Sojisuporn et al., 2010) may also promote the genetic exchange. The close similarity of Malaysian strains to those of Indonesia may also be explained by the seasonal currents in the Malay Peninsula (Tangang et al., 2011).

Prorocentrum concavum from the Caribbean Sea was reported to generate okadaic acid and diol esters of okadaic acid (Dickey et al., 1990; Hu et al., 1992). However, strain TIO941 from Indonesia does not

Table 3

LSU rDNA (D1–D3) sequence differences (above the diagonal line) and similarity (below the diagonal line) of *Prorocentrum fukuyoi.*

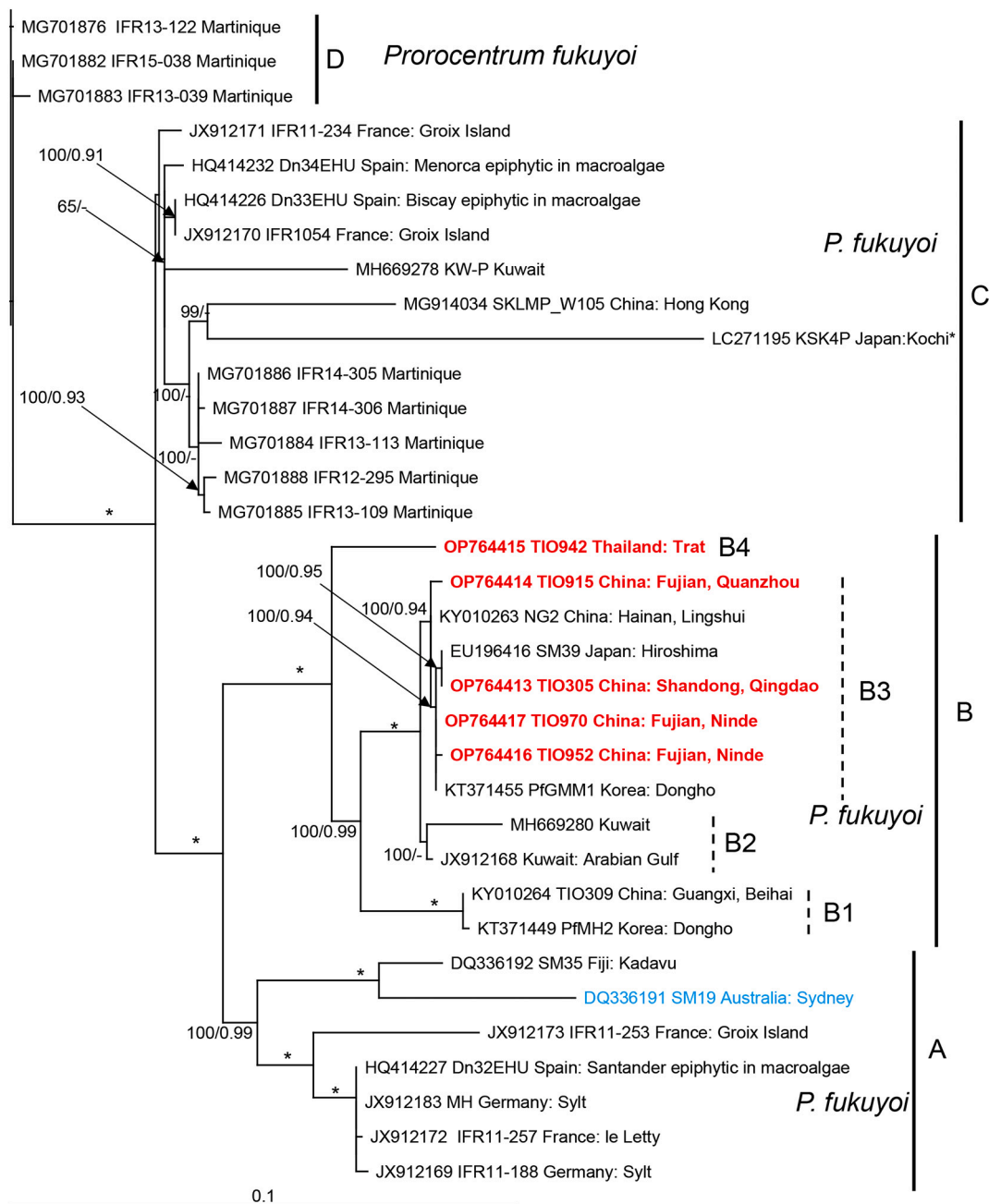|	GenBank no/Strains, origin	1	2	3	4	5	6	7	8	9
1	OP764413/TIO305, Yellow Sea	–	1	4	30	37	54	70	89	195
2	OP764417/TIO970, East China Sea	99.80%	–	3(280 km)	31	36	53	69	88	194
3	OP764414/TIO915, East China Sea	99.50%	99.60%	–	32	37	54	70	89	195
4	KY010264/South China Sea	96.40%	96.30%	96.20%	–	39	63	76	95	201
5	OP764415/TIO942, Gulf of Thailand	95.60%	95.70%	95.60%	95.40%	–	55	69	89	196
6	JX912183/MH, North Sea	93.60%	93.70%	93.60%	92.60%	93.50%	–	63	74	192
7	MG701888/IFR12–295, Martinique)	91.90%	92.10%	91.90%	91.30%	92.10%	92.70%	–	98	148
8	DQ336191/SM19, Sydney	89.50%	89.60%	89.50%	88.90%	89.50%	91.20%	88.80%	–	216
9	LC271195/KSK4P, Japan	77.70%	77.80%	77.70%	77.10%	77.60%	78.10%	83.10%	0.753	–

Fig. 8. A maximum likelihood (ML) inferred tree of *Prorocentrum fukuyoi* based on sequences of LSU rRNA gene (D1–D3). Red and bold nodal labels refer to newly obtained sequences. Lengths of branches are painted to scale. The scale bar is equal to the number of nucleotide substitutions per site. Nodal supports are ML bootstrap support (BS) and Bayesian inference posterior probabilities (BI PP). BS <50% and PP <0.9 are not shown. Asterisk refers to maximal support (ML BS: 100; BI PP: 1.0).

Table 4
LSU rDNA (D1–D3) sequence differences (above the diagonal line) and similarity (below the diagonal line) of *Prorocentrum mexicanum*.

|	GenBank no/Strains, origin	1	2	3	4	5	6	7	8	9
1	OP764422/TIO241, East China Sea	–	0	0	0	1	2	4	5	7
2	OP764424/TIO603, Gulf of Thailand	100%	–	0	0	1	2	4	5	7
3	HF565183/PRJJ3, Korea	100%	100%	–	0	1	2	4	5	7
4	KY426837/Brazil	100%	100%	100%	–	1	2	4	5	7
5	FJ842097/NMN016,Spain	99.80%	99.80%	99.80%	99.80%	–	3	5	6	8
6	AJ567468/PMeRN_01, Reunion	99.70%	99.70%	99.70%	99.70%	99.60%	–	6	7	9
7	JQ616822/PXPV-1,Mexico	99.40%	99.40%	99.40%	99.40%	99.30%	99.20%	–	9	11
8	MW177930/CAWD153,Australia	99.30%	99.30%	99.30%	99.30%	99.20%	99.10%	98.80%	–	10
9	MH669284/Kuwait	99.10%	99.10%	99.10%	99.10%	98.90%	98.80%	98.60%	98.70%	–
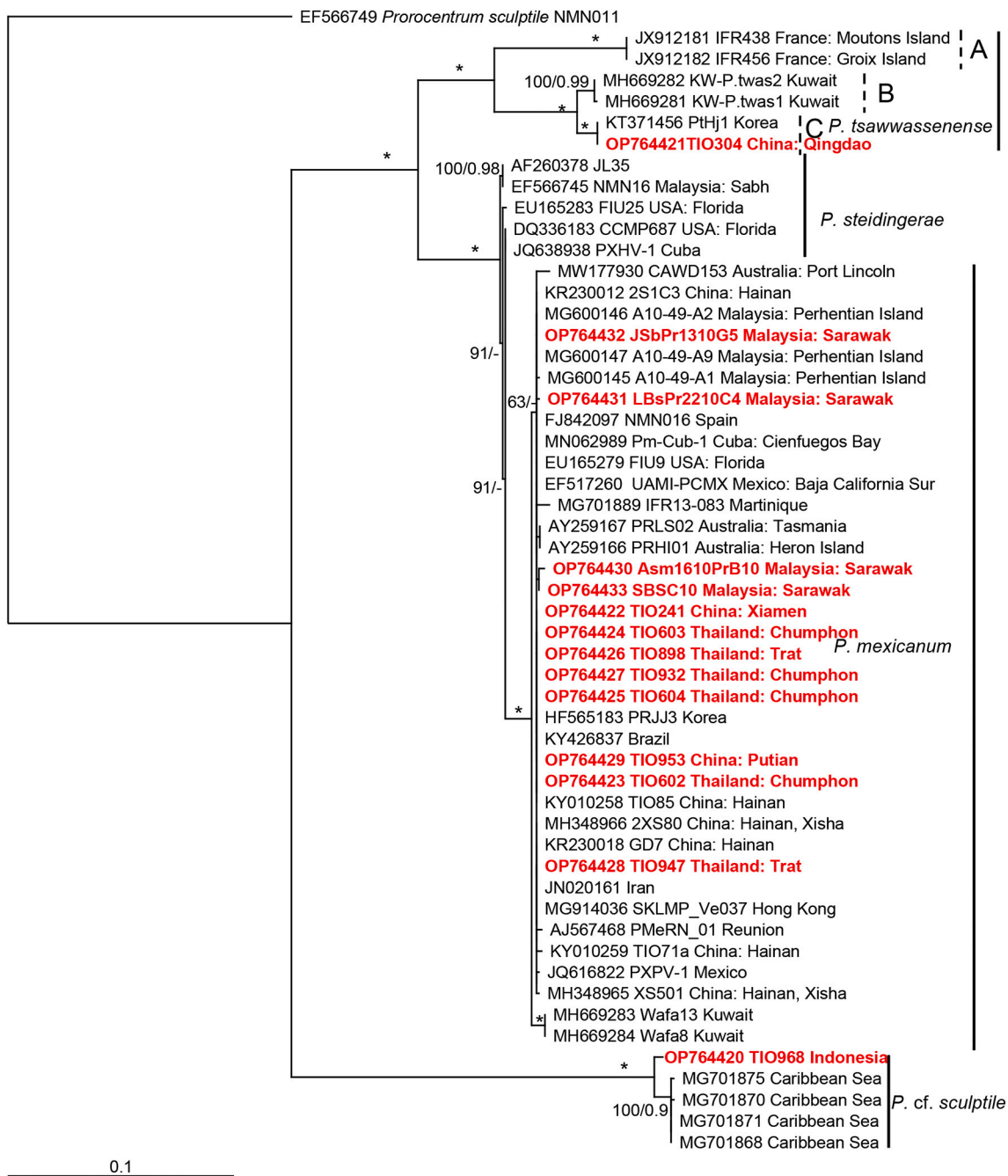
Fig. 9. A maximum likelihood (ML) inferred tree of *Prorocentrum mexicanum, P.* cf. *sculptile* and *P. tsawwassenense* based on sequences of LSU rRNA gene (D1–D3). Red and bold nodal labels refer to newly obtained sequences. Lengths of branches are painted to scale. The scale bar is equal to the number of nucleotide substitutions per site. Nodal supports are ML bootstrap support (BS) and Bayesian inference posterior probabilities (BI PP). BS <50% and PP <0.9 are not shown. Asterisk refers to maximal support (ML BS: 100; BI PP: 1.0).

Table 5
LSU rDNA (D1–D3) sequence differences (above the diagonal line) and similarity (below the diagonal line) of *Prorocentrum tsawwassenense* and *P.* cf. *sculptile.*

Species	GenBank no/Strains, origin	TIO968	MG701873	TIO304	KT371456	MH669282	MH669281	JX912182	JX912181
P. cf. *sculptile*	OP764420/TIO968, Indonesia	–	14	261	444	257	259	230	230
P. cf. *sculptile*	MG701873/Caribbean Sea	98.30%	–	262	444	258	260	232	232
P. tsawwassenense	OP764421/TIO304, Qingdao	71.90%	71.80%	–	1	16	19	114	114
P. tsawwassenense	KT371456/Korea	52.30%	52.30%	99.90%	–	14	14	96	96
P. tsawwassenense	MH669282/Kuwait	72.30%	72.20%	98.20%	97.90%	–	3	116	116
P. tsawwassenense	MH669281/Kuwait	72.10%	72.00%	97.90%	97.90%	99.60%	–	118	118
P. tsawwassenense	JX912182/France	74.30%	74.00%	87.60%	86.20%	87.40%	87.20%	–	1
P. tsawwassenense	JX912181/France	74.30%	74.00%	87.60%	86.20%	87.40%	87.20%	99.80%	–

Table 6
Occurrence of *Prorocentrum* species in different climate zones (+: present; −: absent).

Species/ribotypes	Temperate (station 1 in Fig. 1)	Subtropical (stations 2–6 in Fig. 1)	Tropical (stations 7–12 in Fig. 1)
P. tsawwassenense ribotype C	+	−	−
P. fukuyoi ribotype B3	+	+	−
P. fukuyoi ribotype B4	−	−	+
P. cf. *sculptile*	−	−	+
P. concavum ribotype A	−	−	+
P. concavum ribotype B	−	−	+
P. concavum ribotype C	−	+	−
P. mexicanum	−	+	+

produce detectable toxins, consistent with previous findings on strains from Hainan, China, and Australia (Luo et al., 2017; Verma et al., 2019; Zou et al., 2021). Toxin production might serve to differentiate strains of different origins.

4.1.2. Prorocentrum fukuyoi

Prorocentrum fukuyoi is very similar to *P. emarginatum* but has a narrower valve and a less pronounced spine, and the pores are sparser, thus the pore pattern is not clearly radiating in *P. fukuyoi* (Fukuyo, 1981; Murray et al., 2007; Hoppenrath et al., 2013). Our cells fit the original descriptions of *P. fukuyoi*, but are genetically distant from the type material of Australia. However, strain TIO305 from Qingdao, China shares an identical sequence with strain SM39 from Hiroshima, Japan. The latter was identified as *P. fukuyoi* as well during the original description (Murray et al., 2007), but its sequence was not included in their molecular phylogeny. Our result, however, clearly demonstrates that these strains fell within a separate clade (ribotype B) from the type material.

The morphology of strains from ribotype C appears variable. Strains Dn34EHU from Brazil (Laza-Martinez et al., 2011), KSK4P from Japan also fit the original description in terms of the sparse pores (Nishimura et al., 2020b), but strains Dn33EHU from Brazil (Laza-Martinez et al., 2011), IFR13–113 from the Caribbean Sea show dense pores (Chomérat et al., 2018). The molecular sequences of true *P. emarginatum* are still not available, therefore, these strains have been named *P.* cf. *fukuyoi* or *P. emarginatum/fukuyoi* complex tentatively (Laza-Martinez et al., 2011; Chomérat et al., 2018).

The strain KSK4P from Japan was reported to produce okadaic acid (Nishimura et al., 2020b), which was classified within ribotype C (Fig. 9). Toxin production by strains of other ribotypes will be interesting to investigate and may serve to differentiate clades.

4.1.3. Prorocentrum mexicanum

Our strains of *P. mexicanum* fit the original description regarding cell size, shape, periflagellar plates, and distinctive radially arranged pores (Loeblich et al., 1979). *P. mexicanum* is morphologically and genetically close to *Prorocentrum steidingerae* but can be separated by the smooth surface instead of rugose surface (Gómez et al., 2017).

The failure to detect okadaic acid in *P. mexicanum* strains TIO214 and TIO497 from the East China Sea and Gulf of Thailand is consistent with the previous survey on strains from the Mediterranean Sea (Aligizaki et al., 2009), northern South China Sea (Luo et al., 2017), Malay Peninsula (Lim et al., 2019). *P. mexicanum/rhathymum* strains FIU25 and NMN016 from Florida, USA, and Sabah, Malaysia have been reported to produce okadaic acid (An et al., 2010; Caillaud et al., 2010) but these strains turned out to be *P. steidingerae* instead (Gómez et al., 2017). An

Indian strain of *P. mexicanum* was reported to produce dinophysistoxin-1 (DTX1) but no detectable okadaic acid (Naik et al., 2018). The molecular sequence of this strain is not available thus its true identity remains to be determined.

4.1.4. Prorocentrum tsawwassenense and Prorocentrum cf. sculptile

P. tsawwassenense has been reported in British Columbia, Canada (Hoppenrath and Leander, 2008) and later in France, Kuwait, and Korea (Hoppenrath et al., 2013; Kim et al., 2015). Here we report this species in the Chinese waters for the first time.

P. sculptile was described from Belize (Faust, 1994), but it is morphologically close to *P. emarinatum*, originally isolated from the Ryukyu Island, Japan (Fukuyo, 1981). These two species share a deep V-shaped periflagellar area, numerous depressions and radially arranged pores (Chomérat et al., 2018). Strain TIO968 share 98.30% similarity with *P.* cf. *sculptile* from the Caribbean Sea and they are morphologically close too in terms of a V-shaped periflagellar area, numerous depressions and pore arrangement (Chomérat et al., 2018). Toxin of these two species have not been reported before.

4.2. Potential ecological indicator for climate changes

The use of ecological indicators to monitor environmental changes is often reliable and cost-effective, but applications of ecological indicators in early warnings of environmental change and assessment of climate change is still rare (Siddig et al., 2016). Selection of ecological indicators in marine environment is challenging as many species do not have the barrier for dispersal. However, the benthic *Prorocentrum* species are advantageous as ecological indicators for clime change since they have slow dispersal potential. Among five studied species, *P. tsawwassenense* and *P.* cf. *sculptile* are rarely found (Fig. S1), thus do not meet the requirement of ecolocial indicator, meaning that they must be easily monitored (Dale and Beyeler, 2001).

Prorocentrum mexicanum was only recorded in tropical and subtropical areas here (Table 6), but it was reported in temperate areas too (e.g. Korea, Lim et al., 2013), thus are not suitable ecological indicators for climate change. *P. mexicanum* was reported as an epiphytic or tychoplanktonic species (Aligizaki et al., 2009; Gómez et al., 2017), which even formed blooms (Thomas et al., 2021). The planktonic behavior may explain its wide distribution in the Western Pacific as it is easier to be transported by costal currents.

Natural dispersal through currents may explain the sympatric occurrence of *P. concavum* clades A and B in Sabah, Malaysia, and Caribbean Sea. Sympatric speciation could not be excluded, but long-distance dispersal via their substrates is more likely as shown in several invertebrates on kelp rafts (Waters et al., 2018). However, these potential dispersal events are nearly horizontal which occurred within the same climate zone. *P. concavum* is distributed in tropical and sub-tropical areas only (Fig. S1), thus the East China Sea may act as the sentinel area for monitoring its dispersal as a response to climate change.

Like *P. concavum*, co-occurrence of *P. fukuyoi* ribotypes was found in several localities, eg., Kuwait, Froix Island of France, which may be explained by the epiphytic behavior (Laza-Martinez et al., 2011) and natural dispersal. *P. fukuyoi* was encountered across the Western Pacific (Fig. S2), but strains with various geographic origins showed detectable molecular differentiation, thus is recommended as the candidate for ecological indicator, too. Likewise, the East China Sea may act as the sentinel area as it harbours several genetically differentiated populations. A single species is not sufficient to reflect the complexity of the total environment (Lindenmayer and Likens, 2011), therefore, a combination of several benthic species will greatly improve the sensibility and reliability to detect the environmental changes.

Ballast water has been supposed to play an important role in dinophyte dispersal, especially those producing resting cysts as they are able to survive long term darkness (Hallegraeff, 1998). However, only one *Prorocentrum* species (*P. leve*) is known to have a cyst stage (Mertens

et al., 2017), thus the ballast water assisted dispersal might not apply to *Prorocentrum* species.

Previous work on the response of phytoplankton to climate changes have already shown the poleward dispersal (Nehring, 1998; Kremp et al., 2019). These conclusions are based on long-term monitoring of species presence but the possible cryptic diversity within species was neglected. For instance, *Alexandrium minutum* in the North Sea was postulated as an invasion from the Mediterranean Sea (Nehring, 1998), but it is now known that there are at least four ribotypes within *A. minutum* (Liu et al., 2022). More careful examinations are needed to verify the previous hypothesis.

Our results show that one base pair mutation in the LSU rRNA gene may occur within populations of *P. concavum* or *P. fukuyoi* 80 km away, thus providing a sound basis to infer the potential dispersal. Molecular marker with higher resolution such as microsatellite has been applied to trace the dispersal of sea star (Zulliger et al., 2009), but this approach is much more complex compared to ribosomal DNA sequencing.

It is hard to know if poleward dispersal of benthic *P. fukuyoi* and *P. concavum* is taking place. More intensive sampling is necessary and more isolates need to be sequenced. This approach, however, is time-consuming, therefore metabarcoding will be more efficient to reveal the past dispersal. Such an approach has been applied to uncover sand-dwelling species targeting the conserved 18S rRNA (Reñé et al., 2021). To fulfill this purpose, a more variable region such as LSU rRNA will be a better choice as it has proven powerful to reveal the diversity of dinophytes, even to the ribotype level (Fu et al., 2021).

Declaration of Competing Interest

The authors declare that they have no known competing financial interests or personal relationships that could have appeared to influence the work reported in this paper.

Data availability

Data will be made available on request.

Acknowledgements

Appendix A. Supplementary data

Supplementary data to this article can be found online at https://doi.org/10.1016/j.seares.2022.102304.

References

Aligizaki, K., Nikolaidis, G., Katikou, P., Baxevanis, A.D., Abatzopoulos, T.J., 2009. Potentially toxic epiphytic *Prorocentrum* (Dinophyceae) species in Greek coastal waters. Harmful Algae 8, 299–311.

An, T., Winshell, J., Scorzetti, G., Fell, J.W., Rein, K.S., 2010. Identification of okadaic acid production in the marine dinoflagellate *Prorocentrum rhathymum* from Florida Bay. Toxicon 55, 653–657.

Anderson, D.M., Fachon, E., Pickart, R.S., Lin, P., Fischer, A.D., Richlen, M.L., Uva, V., Brosnahan, M.L., Mcraven, L., Bahr, F., 2021. Evidence for massive and recurrent toxic blooms of *Alexandrium catenella* in the Alaskan Arctic. PNAS 118, e2107387118.

Boc, A., Diallo, A.B., Makarenkov, V., 2012. T-REX: a web server for inferring, validating and visualizing phylogenetic trees and networks. Nucleic Acids Res. 40, W573–W579.

Brown, J.H., Stevens, G.C., Kaufman, D.M., 1996. The geographic range: size, shape, boundaries, and internal structure. Annu. Rev. Ecol. Syst. 27, 597–623.

Burger, J., 2006. Bioindicators: types, development, and use in ecological assessment and research. Environ. Bioindic. 1, 22–39.

Caillaud, A., De La Iglesia, P., Campàs, M., Elandaloussi, L., Fernández, M., Mohammad-Noor, N., Andree, K., Diogène, J., 2010. Evidence of okadaic acid production in a cultured strain of the marine dinoflagellate *Prorocentrum rhathymum* from Malaysia. Toxicon 55, 633–637.

Chomérat, N., Bilien, G., Zentz, F., 2018. A taxonomical study of benthic *Prorocentrum* species (Prorocentrales, Dinophyceae) from Anse Dufour (Martinique Island, eastern Caribbean Sea). Mar. Biodivers. 49, 1299–1319.

Dale, V.H., Beyeler, S.C., 2001. Challenges in the development and use of ecological indicators. Ecol. Indic. 1 (1), 3–10.

Dickey, R.W., Bobzin, S.C., Faulkner, D.J., Bencsath, F.A., Andrzejewski, D., 1990. Identification of okadaic acid from a Caribbean dinoflagellate, *Prorocentrum concavum*. Toxicon 28, 371–377.

Drouet, K., Jauzein, C., Herviot-Heath, D., Hariri, S., Laza-Martinez, A., Lecadet, C., Plus, M., Seoane, S., Sourisseau, M., Lemée, R., 2021. Current distribution and potential expansion of the harmful benthic dinoflagellate *Ostreopsis* cf. *siamensis* towards the warming waters of the Bay of Biscay, North-East Atlantic. Environ. Microbiol. 23, 4956–4979.

Faust, M., 1990. Morphologic details of six benthic species of *Prorocentrum* (Pyrrophyta) from a mangrove island, Twin Cays, Belize, including two new species. J. Phycol. 26, 548–558.

Faust, M., 1993. Three new benthic species of *Prorocentrum* (Dinophyceae) from Twin Cays, Belize: *P. maculosum* sp. nov., *P. foraminosum* sp. nov. and *P. formosum* sp. nov. Phycologia 32, 410–418.

Faust, M.A., 1994. Three new benthic species of *Prorocentrum* (Dinophyceae) from Carrie Bow Cay, Belize: *P. sabulosum* sp. nov., *P. sculptile* sp. nov., and *P. arenarium* sp. nov. J. Phycol. 30, 755–763.

Faust, M.A., Vandersea, M.W., Kibler, S., Tester, P.A., Litaker, R.W., 2008. *Prorocentrum levis*, a new benthic species (Dinophyceae) from a mangrove island, twin cays, Belize. J. Phycol. 44, 232–240.

Fu, Z., Piumsomboon, A., Punnarak, P., Uttayarnmanee, P., Leaw, C.P., Lim, P.T., Wang, A., Gu, H., 2021. Diversity and distribution of harmful microalgae in the Gulf of Thailand assessed by DNA metabarcoding. Harmful Algae 106, 102063.

Fukuyo, Y., 1981. Taxonomical study on benthic dinoflagellates collected in coral reefs. Bull. Jap. Soc. Sci. Fish. 47, 967–978.

Gómez, F., Qiu, D., Lin, S., 2017. The synonymy of the toxic dinoflagellates *Prorocentrum mexicanum* and *P. rhathymum* and the description of *P. steidingerae* sp. nov. (Prorocentrales, Dinophyceae). J. Eukaryot. Microbiol. 64, 668–677.

Grzebyk, D., Sako, Y., Berland, B., 1998. Phylogenetic analysis of nine species of *Prorocentrum* (Dinophyceae) inferred from 18s ribosomal DNA sequences, morphological comparisons, and description of *Prorocentrum panamensis*, sp. nov. J. Phycol. 34, 245–264.

Guillard, R.R.L., Ryther, J.H., 1962. Studies of marine planktonic diatoms. I. *Cyclotella nana* Hustedt and *Detonula confervacea* Cleve. Can. J. Microbiol. 8, 229–239.

Guiry, M.D., Guiry, G.M., 2022. AlgaeBase. World-Wide Electronic Publication. National University of Ireland, Galway. https://www.algaebase.org. searched on March 26, 2022.

Hall, T.A., 1999. BioEdit: A User-Friendly Biological Sequence Alignment Editor and Analysis Program for Windows 95/98/NT. ed. N.a.S. Series, pp. 95–98.

Hallegraeff, G.M., 1998. Transport of toxic dinoflagellates via ships ballast water: bioeconomic risk assessment and efficacy of possible ballast water management strategies. Mar. Ecol. Prog. Ser. 168, 297–309.

Hoppenrath, M., 2000. A new marine sand-dwelling *Prorocentrum* species, *P. clipeus* sp. nov. (Dinophyceae, Prorocentrales) from Helgoland, German Bight, North Sea. Eur. J. Protistol. 36, 29–33.

Hoppenrath, M., Leander, B.S., 2008. Morphology and molecular phylogeny of a new marine sand-dwelling *Prorocentrum* species, *P. tsawwassenense* (dinophyceae, prorocentrales), from British Columbia, Canada. J. Phycol. 44, 451–466.

Hoppenrath, M., Chomérat, N., Horiguchi, T., Schweikert, M., Nagahama, Y., Murray, S., 2013. Taxonomy and phylogeny of the benthic *Prorocentrum* species (Dinophyceae)—a proposal and review. Harmful Algae 27, 1–28.

Hu, T., Marr, J., De Freitas, A.S., Quilliam, M.A., Walter, J.A., Wright, J.L., Pleasance, S., 1992. New diol esters isolated from cultures of the dinoflagellates *Prorocentrum lima* and *Prorocentrum concavum*. J. Nat. Prod. 55, 1631–1637.

Katoh, K., Standley, D.M., 2013. MAFFT multiple sequence alignment software version 7: improvements in performance and usability. Mol. Biol. Evol. 30, 772–780.

Kim, S., Yoon, J., Park, M.G., 2015. Occurrence and molecular phylogenetic characteristics of benthic sand-dwelling dinoflagellates in the intertidal flat of Dongho, west coast of Korea. Sea J. Korean Soc. Oceanogr. 20, 141–150.

Kremp, A., Hansen, P.J., Tillmann, U., Savela, H., Suikkanen, S., Voß, D., Barrera, F., Jakobsen, H.H., Krock, B., 2019. Distributions of three *Alexandrium* species and their toxins across a salinity gradient suggest an increasing impact of GDA producing *A. pseudogonyaulax* in shallow brackish waters of Northern Europe. Harmful Algae 87, 101622.

Krock, B., Tillmann, U., John, U., Cembella, A., 2008. LC-MS-MS aboard ship: tandem mass spectrometry in the search for phycotoxins and novel toxigenic plankton from the North Sea. Anal. Bioanal. Chem. 392, 797–803.

Larsen, J., Nguyen, N., 2004. Potentially toxic microalgae of Vietnamese waters. Opera Bot. 140, 5–216.

Laza-Martinez, A., Orive, E., Miguel, I., 2011. Morphological and genetic characterization of benthic dinoflagellates of the genera *Coolia, Ostreopsis* and *Prorocentrum* from the South-Eastern Bay of Biscay. Eur. J. Phycol. 46, 45–65.

Lim, A.S., Jeong, H.J., Jang, T.Y., Kang, N.S., Lee, S.Y., Yoo, Y.D., Kim, H.S., 2013. Morphology and molecular characterization of the epiphytic dinoflagellate *Prorocentrum* cf. *rhathymum* in temperate waters off Jeju Island, Korea. Ocean Sci. J. 48, 1–17.

Lim, Z.F., Luo, Z., Lee, L.K., Hii, K.S., Teng, S.T., Chan, L.L., Chomérat, N., Krock, B., Gu, H., Lim, P.T., Leaw, C.P., 2019. Taxonomy and toxicity of *Prorocentrum* from Perhentian Islands (Malaysia), with a description of a non-toxigenic species *Prorocentrum malayense* sp. nov. (Dinophyceae). Harmful Algae 83, 95–108.

Lindenmayer, D.B., Likens, G.E., 2011. Direct measurement versus surrogate indicator species for evaluating environmental change and biodiversity loss. Ecosystems 14, 47–59.

Liu, M., Krock, B., Yu, R., Leaw, C.P., Lim, P.T., Ding, G., Wang, N., Zheng, J., Gu, H., 2022. Co-occurrence of *Alexandrium minutum* (Dinophyceae) ribotypes from the Chinese and Malaysian coastal waters and their toxin production. Harmful Algae 115, 102238.

Loeblich, A.R., Sherley, J.L., Schmidt, R.J., 1979. The correct position of flagellar insertion in *Prorocentrum* and description of *Prorocentrum rhathymum* sp. nov. (Pyrrhophyta). J. Plankton Res. 1, 113–120.

Luo, Z., Zhang, H., Krock, B., Lu, S., Yang, W., Gu, H., 2017. Morphology, molecular phylogeny and okadaic acid production of epibenthic *Prorocentrum* (Dinophyceae) species from the northern South China Sea. Algal Res. 22, 14–30.

Masson-Delmotte, V., Zhai, P., Pirani, A., Connors, S.L., Péan, C., Berger, S., Caud, N., Chen, Y., Goldfarb, L., Gomis, M.I., 2021. In: Masson-Delmotte, V., Zhai, P., Pirani, A., Connors, S.L., Péan, C., Berger, S., Caud, N., Chen, Y., Goldfarb, L., Gomis, M.I., Huang, M., Leitzell, K., Lonnoy, E., Matthews, J.B.R., Maycock, T.K., Waterfield, T., Yelekçi, O., Yu, R., Zhou, B. (Eds.), IPCC, 2021: Summary for Policymakers. In: Climate Change 2021: The Physical Science Basis. Contribution of Working Group I to the Sixth Assessment Report of the Intergovernmental Panel on Climate Change. Cambridge University Press IPCC, Geneva, Switzerland.

Mertens, K.N., Gu, H., Pospelova, V., Chomérat, N., Nézan, E., Gurdebeke, P.R., Bogus, K., Vrielinck, H., Rumebe, M., Meteigner, C., 2017. First record of resting cysts of the benthic dinoflagellate *Prorocentrum leve* in a natural reservoir in Gujan-Mestras, Gironde, France. J. Phycol. 53 (6), 1193–1205.

Mohammad-Noor, N., Daugbjerg, N., Moestrup, Ø., Anton, A., 2007a. Marine epibenthic dinoflagellates from Malaysia–A study of live cultures and preserved samples based on light and scanning electron microscopy. Nord. J. Bot. 24, 629–690.

Mohammad-Noor, N., Moestrup, Ø., Daugbjerg, N., 2007b. Light, electron microscopy and DNA sequences of the dinoflagellate *Prorocentrum concavum* (syn. *P. arabianum*) with special emphasis on the periflagellar area. Phycologia 46, 549–564.

Morton, S.L., Bomber, J.W., 1994. Maximizing okadaic acid content from *Prorocentrum hoffmannianum* Faust. J. Appl. Phycol. 6, 41–44.

Morton, S.L., Moeller, P.D., Young, K., Lanoue, B., 1998. Okadaic acid production from the marine dinoflagellate *Prorocentrum belizeanum* Faust isolated from the Belizean coral reef ecosystem. Toxicon 36, 201–206.

Morton, S.L., Faust, M.A., Fairey, E.A., Moeller, P.D., 2002. Morphology and toxicology of *Prorocentrum arabianum* sp. nov.,(Dinophyceae) a toxic planktonic dinoflagellate from the Gulf of Oman, Arabian Sea. Harmful Algae 1, 393–400.

Murakami, Y., Oshima, Y., Yasumoto, T., 1982. Identification of okadaic acid as a toxic component of a marine dinoflagellate *Prorocentrum lima*. Bull. Jap. Soc. Sci. Fish. (Japan) 48, 69–72.

Murray, S., Nagahama, Y., Fukuyo, Y., 2007. Phylogenetic study of benthic, spine-bearing prorocentroids, including *Prorocentrum fukuyoi* sp. nov. Phycol. Res. 55, 91–102.

Naik, R.K., Damare, S., Yapa, K., D'costa, P.M., Roy, R., 2018. First report of toxic *Prorocentrum rhathymum* (Dinophyceae) and its pigment composition from coastal waters of the eastern Arabian Sea. Indian J. Geo Mar. Sci. 47, 645–652.

Nascimento, S.M., Mendes, M.C.Q., Menezes, M., Rodríguez, F., Alves-De-Souza, C., Branco, S., Riobó, P., Franco, J., Nunes, J.M.C., Huk, M., 2017. Morphology and phylogeny of *Prorocentrum caipirignum* sp. nov. (Dinophyceae), a new tropical toxic benthic dinoflagellate. Harmful Algae 70, 73–89.

Nehring, S., 1998. Establishment of thermophilic phytoplankton species in the North Sea: biological indicators of climatic changes? *ICES.* J. Mar. Sci. 55, 818–823.

Nishimura, T., Uchida, H., Noguchi, R., Oikawa, H., Suzuki, T., Funaki, H., Ihara, C., Hagino, K., Arimitsu, S., Tanii, Y., 2020a. Abundance of the benthic dinoflagellate *Prorocentrum* and the diversity, distribution, and diarrhetic shellfish toxin production of *Prorocentrum lima* complex and *P. caipirignum* in Japan. Harmful Algae 96, 101687.

Nishimura, T., Uchida, H., Suzuki, T., Tawong, W., Abe, S., Arimitsu, S., Adachi, M., 2020b. First report on okadaic acid production of a benthic dinoflagellate *Prorocentrum* cf. *fukuyoi* from Japan. Phycol. Res. 68, 30–40.

Pecl, G.T., Araújo, M.B., Bell, J.D., Blanchard, J., Bonebrake, T.C., Chen, I.-C., Clark, T. D., Colwell, R.K., Danielsen, F., Evengård, B., 2017. Biodiversity redistribution under climate change: impacts on ecosystems and human well-being. Science 355, eaai9214.

Piumsomboon, A., Songroop, C., Tamisanon, C., 2001. Benthic Microalgae in Mangrove and Coastal Ecosystems. National Research Council of Thailand, Bangkok, pp. 1–60.

Poloczanska, E.S., Brown, C.J., Sydeman, W.J., Kiessling, W., Schoeman, D.S., Moore, P. J., Brander, K., Bruno, J.F., Buckley, L.B., Burrows, M.T., 2013. Global imprint of climate change on marine life. Nat. Clim. Chang. 3, 919–925.

Posada, D., 2008. jModelTest: phylogenetic model averaging. Mol. Biol. Evol. 25, 1253–1256.

Reñé, A., Hoppenrath, M., Reboul, G., Moreira, D., López-García, P., 2021. Composition and temporal dynamics of sand-dwelling dinoflagellate communities from three Mediterranean beaches. Aquat. Microb. Ecol. 86, 85–98.

Rodríguez, F., Riobó, P., Crespín, G.D., Daranas, A.H., De Vera, C.R., Norte, M., Fernández, J.J., Fraga, S., 2018. The toxic benthic dinoflagellate *Prorocentrum maculosum* Faust is a synonym of *Prorocentrum hoffmannianum* Faust. Harmful Algae 78, 1–8.

Ronquist, F., Huelsenbeck, J.P., 2003. MrBayes 3: Bayesian phylogenetic inference under mixed models. Bioinformatics 19, 1572–1574.

Saburova, M., Al-Yamani, F., Polikarpov, I., 2009. Biodiversity of free-living flagellates in Kuwait's intertidal sediments. BioRisk 3, 97–110.

Siddig, A.A., Ellison, A.M., Ochs, A., Villar-Leeman, C., Lau, M.K., 2016. How do ecologists select and use indicator species to monitor ecological change? Insights from 14 years of publication in ecological indicators. Ecol. Indic. 60, 223–230.

Sojisuporn, P., Morimoto, A., Yanagi, T., 2010. Seasonal variation of sea surface current in the Gulf of Thailand. Coast. Mar. Sci. 34, 91–102.

Stamatakis, A., 2006. RAxML-VI-HPC: maximum likelihood-based phylogenetic analyses with thousands of taxa and mixed models. Bioinformatics 22, 2688–2690.

Tangang, F.T., Xia, C., Qiao, F., Juneng, L., Shan, F., 2011. Seasonal circulations in the Malay Peninsula Eastern continental shelf from a wave–tide–circulation coupled model. Ocean Dyn. 61, 1317.

Tester, P.A., Litaker, R.W., Berdalet, E., 2020. Climate change and harmful benthic microalgae. Harmful Algae 91, 101655.

Thomas, M.K., Kremer, C.T., Klausmeier, C.A., Litchman, E., 2012. A global pattern of thermal adaptation in marine phytoplankton. Science 338, 1085–1088.

Thomas, L.C., Nandan, S.B., Padmakumar, K., 2021. First report on an unusual bloom of the potentially toxic epibenthic dinoflagellate *Prorocentrum rhathymum* from Bangaram Lagoon of the Lakshadweep archipelago: Arabian Sea. Reg. Stud. Mar. Sci. 41, 101549.

Verma, A., Kazandjian, A., Sarowar, C., Harwood, D.T., Murray, J.S., Pargmann, I., Hoppenrath, M., Murray, S.A., 2019. Morphology and phylogenetics of benthic *Prorocentrum* species (Dinophyceae) from tropical northwestern Australia. Toxins 11, 571.

Waters, J.M., King, T.M., Fraser, C.I., Craw, D., 2018. An integrated ecological, genetic and geological assessment of long-distance dispersal by invertebrates on kelp rafts. Front. Biogeogr. 10, e40888.

Zhang, H., Li, Y., Cen, J., Wang, H., Cui, L., Dong, Y., Lu, S., 2015. Morphotypes of *Prorocentrum lima* (Dinophyceae) from Hainan Island, South China Sea: morphological and molecular characterization. Phycologia 54, 503–516.

Zou, J., Li, Q., Lu, S., Dong, Y., Chen, H., Zheng, C., Cui, L., 2020. The first benthic harmful dinoflagellate bloom in China: morphology and toxicology of *Prorocentrum concavum*. Mar. Pollut. Bull. 158, 111313.

Zou, J., Li, Q., Liu, H., Liu, Y., Huang, L., Wu, H., Qiu, J., Zhang, H., Lü, S., 2021. Taxonomy and toxin profile of harmful benthic *Prorocentrum* (Dinophyceae) species from the Xisha Islands, South China Sea. J. Oceanol. Limnol. https://doi.org/10.1007/s00343-021-1045-6.

Zulliger, D.E., Tanner, S., Ruch, M., Ribi, G., 2009. Genetic structure of the high dispersal Atlanto-Mediterreanean sea star *Astropecten aranciacus* revealed by mitochondrial DNA sequences and microsatellite loci. Mar. Biol. 156, 597–610.